

Downregulation of VEGF expression attenuates malignant biological behavior of C6 glioma stem cells

QINGQUAN LI, GUANQUN QIAO, JUN MA and YINGBIN LI

Department of Neurosurgery, The Second Affiliated Hospital of Nanjing Medical University,
Nanjing 210000, Jiangsu, P.R. China

Received December 29, 2013; Accepted February 14, 2014

DOI: 10.3892/ijo.2014.2331

Abstract. Several lines of direct evidence show that gliomas express high levels of vascular endothelial growth factor (VEGF). VEGF can promote the growth of gliomas through angiogenesis. It is believed that gliomas originate in the brain tumor stem cells (BTSCs). However, the direct effect of VEGF on the biological behavior of BTSCs has not been completely elucidated. In this study, we established C6 glioma stem cells (C6GSCs) from the C6 glioma cells. Furthermore, we suppressed the VEGF expression of C6GSCs using lentiviral vector-VEGF shRNA. After transfection, the VEGF expression of C6GSCs was downregulated significantly. The proliferation and invasion capacity of transfected C6GSCs was impaired and the ability of differentiation was enhanced. The data demonstrate that downregulation of VEGF expression attenuates malignant biological behavior of C6GSCs. RNA interference of VEGF expression implies an effective anti-gliomas strategy.

Introduction

Gliomas are the most common primary tumors originating in the central nervous system (CNS) (1). They are graded from I to IV based on their degrees of malignancy. The grade IV glioblastoma (GB) is the most common and most malignant type of glioma which is highly invasive, and currently there exists no cure. This could in part be due to the existence of so-called brain tumor stem cells (BTSCs), a cellular subfraction within GB which contribute to recurrent tumor growth and resistance to drugs and irradiation (2). BTSCs exhibit the ability to self-renew as well as give rise to differentiated tissue cells, which are responsible for the progress of a tumor.

Several studies have shown that angiogenesis is essential for glioma growth and metastases (3,4). Vascular endothelial growth factor (VEGF) is the most important stimulant factor in regulating angiogenesis. VEGF, a diffusible 36-46-kDa

glycoprotein (5,6), and has been shown to be a potent mediator of brain tumor angiogenesis, vascular permeability and gliomas growth (7). Several lines of direct evidence show that gliomas and BTSCs express high levels of VEGF (8-11). VEGF secreted by tumor cells interacts with VEGF receptors (VEGFRs) and stimulates downstream signaling molecules such as Akt and mitogen-activated protein kinases (MAPKs) to promote the migration, growth and survival of endothelial cells (12-14).

VEGFRs include two tyrosine kinase receptors, VEGFR-1 and VEGFR-2 (15-18). Traditionally, VEGFRs were thought to be expressed on the surface of tumor endothelial cells, but not on tumor cells (18-20). However, recent studies suggest that tumor-derived VEGF provides not only paracrine survival cues for endothelial cells, but may also fuel autocrine processes in gliomas cells (tumor-secreted VEGF providing prosurvival signaling through VEGFRs expressed by tumor cells or BTSCs themselves) and play a role in tumor resistance to existing therapies (21-24).

However, the direct effect of VEGF on biological behavior of BTSCs has not been completely elucidated. In this study, we established C6 glioma stem cells (C6GSCs), and then the VEGF expression of C6GSCs was downregulated by lentiviral vector-VEGF short hairpin RNA (shRNA). The proliferation, differentiation and invasion of C6GSCs were detected by an inverted phase contrast microscope, flow cytometry and immunofluorescence.

Materials and methods

Isolation and identification of C6GSCs. C6 glioma cells were purchased from the Shanghai Institute of Biochemistry and Cell Biology (Shanghai, China). The cells were cultured in the serum containing medium composed of Dulbecco's modified Eagle's medium (DMEM) with high glucose and 10% fetal bovine serum. Cells that were in the exponential growth phase were then collected and transplanted to a new culture flask with an equal volume of serum-free neural stem cell (NSC) medium containing DMEM/F12 with 2% B27, epidermal growth factor (EGF, 10 ng/ml) and basic fibroblast growth factor (bFGF, 10 ng/ml). Cells were incubated at 37°C with 95% air, 5% CO₂ and 100% humidity. Two weeks later, floating primary tumor spheres were collected. The sphere cells were harvested, dissociated into single cells, and plated into a 96-well plate for

Correspondence to: Dr Yingbin Li, Department of Neurosurgery, The Second Affiliated Hospital of Nanjing Medical University, 121 Jiangjiayuan Road, Nanjing 210000, Jiangsu, P.R. China
E-mail: yixinntu@foxmail.com

Key words: gliomas, vascular endothelial growth factor, brain tumor stem cells, C6 glioma stem cells

the subsphere-forming assay by limiting dilution as described previously (25). In brief, the cells in single-cell suspension were diluted to one cell per microliter and plated at one to two cells per well. Cells were fed with 200 μ l serum-free media with growth factors, changing half of the medium every 5 days. After plating, the cells were observed, and only wells containing a single cell were considered.

Subspheres from one mother cell were characterized by immunocytochemistry against anti-CD133 antibody (1:400, Roche, Germany) or anti-nestin antibody (1:1,000, Chemicon) as described previously. In brief, the subspheres were incubated with primary antibodies: rat anti-CD133, mouse monoclonal anti-nestin overnight at 4°C, followed by incubation with Alexa Fluor 568-conjugated goat anti-rat (1:1,000, Molecular Probes), 488-conjugated goat anti-mouse (1:800, invitrogen). Cell nuclei were counter-stained with Hoechst 33342 for 30 min at room temperature (RT). Immunopositive cells were observed using a fluorescent microscope.

Construction and identification of shRNA lentiviral vector targeting rat VEGF. Four self-complementary hairpin DNA oligos targeting rat VEGF mRNA were designed by using Dharmagon siDESIGN Center algorithm (<http://www.dharmacon.com/DesignCenter/DesignCenterPage.aspx>) as follows: VEGF shRNA1 is 5'-TGCGGATCAAACCTCACC AAA-3'; VEGF shRNA2 is 5'-GAGCGGAGAAAGCATTTG TTT-3'; VEGF shRNA3 is 5'-GCGAGGCAGCTTGAGTTA AAC-3'; VEGF shRNA4 is 5'-GCCTCTGAAACCATGAAC TTT-3', including a 9-nt loop sequences. Also, a mock sequence that lacks any similarity to the rat sequence was designed and synthesized. Lentiviral vectors for rat VEGF shRNA encoding a green fluorescent protein (GFP) sequence and a puromycin resistance gene was constructed by GenePharma (Shanghai, China), named as pGLVH1/GFP/PURO. DNA oligos were annealed and inserted in the rat H1 promoter site of the PGLVH1-GFP vector. Then, the RNA interference (RNAi) cassette was cloned into the latter vector and lentiviral vectors expressing shRNA were constructed. They were then confirmed by DNA sequencing identification.

Lentiviral vector DNAs and packaging vectors (pHelper1.0, pHelper2.0) (Qiagen) were then transfected into 293T cells. After transfection, the cells were incubated at 32°C to increase viral titer. Forty-eight hours later, the supernatant containing the retroviral particles was collected, filtered through the 0.45- μ m low protein binding syringe filter and the titer of lentivirus was determined.

C6GSCs were maintained in above mentioned medium and were plated into 6-well plates at 4×10^5 cells/well. Twenty-four hours later, the cells were transfected with viral supernatants in the presence of polybrene (6 μ g/ml final concentration) for 12 h at a multiplicity of infection (MOI) of 10 and 20, then replaced with a fresh medium containing 5 μ g/ml puromycin. After 72 h, the cells had been transfected for the subsequent study.

Semiquantitative RT-PCR analysis. Total RNA was extracted from 1×10^6 transfected cells in each group using TRIzol reagent (Invitrogen, Carlsbad, CA, USA), and 2 μ g of total RNA was reverse transcribed into cDNA with oligo dT primers using Omniscript reverse transcriptase (Qiagen, Hilden,

Germany) according to the manufacturer's protocol. Hot start PCR was performed to analyze expression levels with the following primers. VEGF: sense 5'-GACCCTGGTGGAC ATCTTCCAGGA-3' and antisense 5'-GGTGAGAGGTCTAG TTCCCGA-3'. GAPDH: sense 5'-TGATGACATCAAGAAG GTGGTGAAG-3' and antisense 5'-TCCTTGGAGGCCAT GTGGGCCAT-3'.

The PCR products were subjected to agarose gel electrophoresis followed by staining with ethidium bromide. The band optical density of VEGF, relative to that of GAPDH (internal control) was quantified by image analysis system (Leica Q550I W, Cambridge, UK).

Western blot analysis. Western blot analysis was performed for whole cell lysate. Aliquots of total protein (50 μ g per lane) were electrophoresed on a 12% SDS-polyacrylamide gradient gel and transferred to nitrocellulose membranes (Millipore). Washed in rinse buffer at RT and incubated in blocking buffer (5% fat-free milk in rinse buffer) for 30 min, the membranes were incubated for 2 h at RT with antibody. Further washed with rinse buffer, the membranes were incubated with 1:1,000 diluted HRP-conjugated secondary antibody (Santa Cruz) for 2 h at RT, followed by developing with enhanced chemiluminescence reagents (Amersham, Little Chalfont Buckinghamshire, UK). In addition, β -actin was used as a reference protein. The optical densities were analyzed by using ImageMaster™ 2D Platinum (Version 5.0, Amersham Biosciences, Piscataway, NJ, USA).

Proliferation assay of C6GSCs. The non-transfected C6GSCs (control group), mock transfected C6GSCs (mock group) and lentiviral vector-VEGF shRNA1 transfected C6GSCs (silence group) were cultured in the above mentioned medium. Photomicrographs were taken by an inverted phase contrast microscope and the size of cell spheres was analyzed. At 7 days *in vitro* (DIV), some cell spheres of three groups were dissociated into single-cell suspension mechanically by trypsin digestion. Collected cells were washed once in cold phosphate-buffered saline (PBS). The cells were fixed in 70% ethanol, treated with 100 mg/l RNase at 37°C for 30 min and stained with 50 mg/l propidium iodide (Sigma) for 30 min. The cells were analyzed using flow cytometry (Epics XL; Beckman Coulter, Fullerton CA, USA).

Differentiation assay of C6GSCs. C6GSCs of three groups (1×10^5 cells/ml) were plated onto poly-D-lysine coated cover slips in 24-well plates containing serum-free medium, respectively. After 7 DIV, cells were fixed with 4% paraformaldehyde (PFA) in 0.1 M phosphate buffer (PB) for 1 h, blocked in 5% goat serum for 30 min at RT and then incubated for 12 h at RT with primary antibodies. After washing three times in PBS, the cells were incubated in secondary antibodies for 6 h at RT. Antibodies were as follows: the primary monoclonal antibodies were against mouse microtubule associated proteins-2 (anti-MAP-2, 1:200, Chemicon), mouse glial fibrillary acidic protein (anti-GFAP, 1:200, Sigma), rat anti-nestin (1:2,000, Millipore). Secondary antibodies were Alexa Fluor 568-conjugated (red) goat anti-mouse IgG (1:500, Invitrogen) or FITC-conjugated (green) goat anti-rat IgG (1:200, Millipore). Cell nuclei were counter-stained with

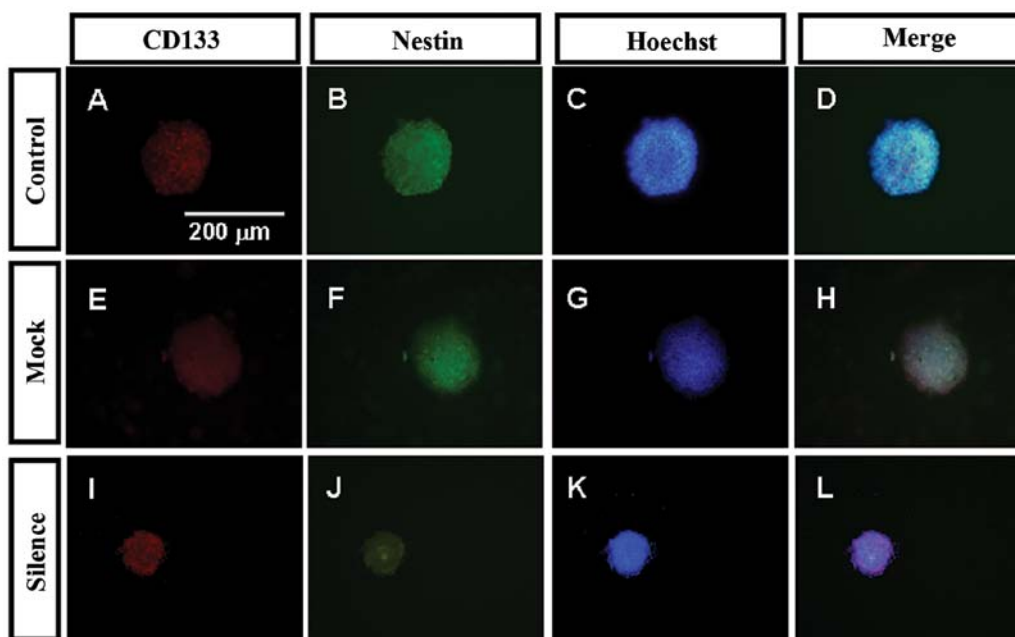


Figure 1. Identification of C6GSCs. C6GSCs were detected by CD133 (red) and nestin (green) immunofluorescence. At 3 DIV, many C6 cells formed floating primary tumor spheres in serum-free NSC medium. Subspheres from one mother cell were CD133 and nestin double-positive. The nestin fluorescence intensity of a C6GSC sphere in the silence group was lower than that of the other two groups.

Hoechst 33342 for 30 min at RT. Immunopositive cells were observed using fluorescent microscopy.

Invasion assay of C6GSCs. C6GSCs of three groups (1×10^5 cells/ml) were added to the upper chamber of the Transwell. The lower chamber was filled with DMEM/F12 medium. After incubation for 12 h at 37°C , the cells were fixed with 4% PFA for 30 min and stained with Hoechst 33342 for 30 min at RT. The filters were then rinsed thoroughly in distilled water and checked by bright field microscopy to ensure that the cells were adherent and had migrated. The non-migrating cells were then removed from the upper surface (inside) of the Transwell with a wet cotton swab.

Statistical analysis. Images were analyzed by Leica Qwin image processing and analysis software (Leica imaging system, Cambridge, UK). Statistical analysis was performed using statistics package for social science 16.0 (SPSS 16.0). Data are presented as mean \pm standard deviation ($M \pm SD$). Statistical comparisons were performed using one-way analysis of variance (ANOVA) and differences at $P < 0.05$ were considered statistically significant.

Results

Identification of C6GSCs. The C6 cells were cultured in serum-free NSC medium, and many formed floating primary tumor spheres. Subspheres from one mother cell were CD133 and nestin double-positive. The nestin fluorescence intensity of the C6GSC sphere of the silence group was lower than that of the other two groups (Fig. 1).

Lentivirus-mediated RNAi inhibits VEGF expression in C6GSCs. In order to exclude an off-target silencing effect

mediated by specific shRNA, we employed 4 different sequences of VEGF shRNA. Lentiviral infection efficiency was calculated by GFP expression under a fluorescence microscope. The infection efficiency of lentiviral vector-shRNA was $98.02 \pm 1.37\%$ when MOI was 1:20 (Fig. 2). To evaluate the inhibition of VEGF mRNA expression, semi-quantitative RT-PCR was performed 72 h after infection, the VEGF mRNA expression in lentiviral vector-VEGF shRNA1 transfected C6GSCs was reduced by $\sim 75\%$, as compared with the non-transfected and mock transfected ones ($P < 0.05$). In addition, no difference was observed among the non-transfected cells, the mock-infected cells, and VEGF shRNA2, 3 and 4 transfected cells (Fig. 3), indicating that the corresponding mRNA sequence for VEGF shRNA1, not VEGF shRNA2, 3 and 4 is specific RNAi target. Western blot analysis was also performed 72 h after infection. The VEGF protein expression demonstrated a significant reduction in lentiviral vector-VEGF shRNA1 transfected C6GSCs, as compared with non-transfected cells and mock transfected cells ($P < 0.05$) (Fig. 4), suggesting that VEGF shRNA1 strongly blocked VEGF expression, whereas no obvious inhibition of VEGF protein was observed in VEGF shRNA2, 3 and 4 transfected cells.

Proliferation of C6GSCs. The C6GSCs of 3 groups were cultured under the same conditions outlined in Materials and methods. The appearance of the sphere of three kinds of stem cells is similar at the beginning, showing a small and uniform cell sphere (Fig. 5A-C). In the following days in culture, non-transfected C6GSCs and mock transfected C6GSC spheres grew significantly faster and reached a larger size than lentiviral vector-VEGF shRNA1 transfected C6GSC spheres (Fig. 5D-I). At 7 DIV, the proliferation of lentiviral vector-VEGF shRNA1 transfected C6GSCs reached the peak. On

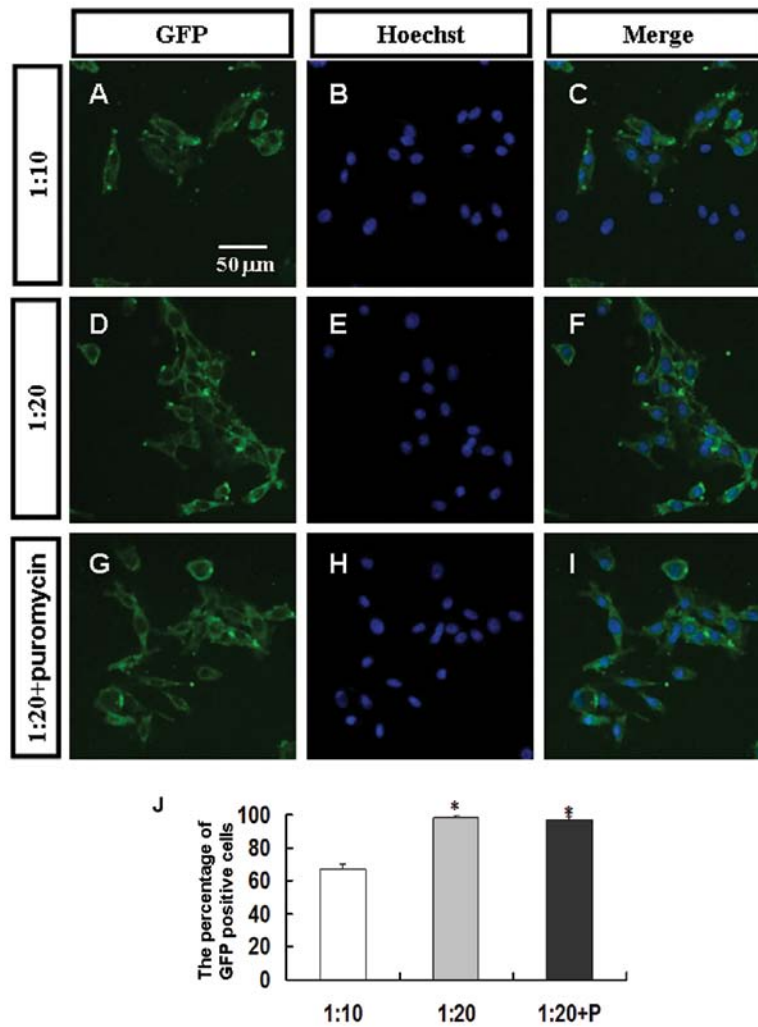


Figure 2. The infection efficiency of lentiviral vector-shRNA. Lentivirus infection efficiency was calculated by GFP expression (green fluorescent protein). The infection efficiency of lentiviral vector-shRNA was 98.02±1.37% at MOI 1:20. * vs. 1:10 P<0.05.

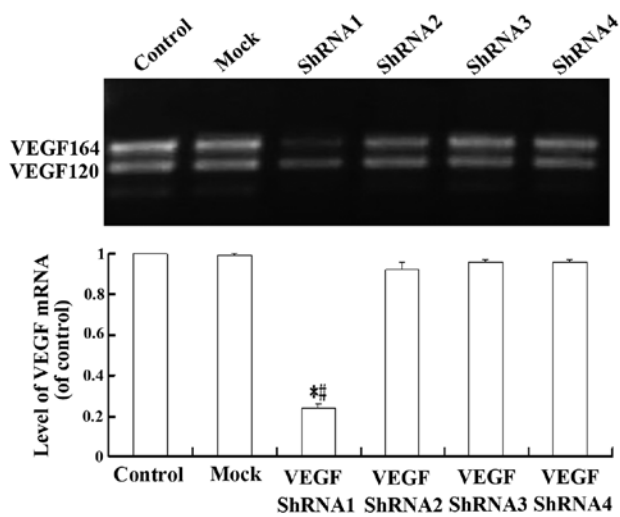


Figure 3. The level of VEGF mRNA was detected by semiquantitative RT-PCR 72 h after infection. The VEGF mRNA expression in lentivirus vector-VEGF shRNA1 transfected C6GSCs cells were reduced by ~75%, as compared with the non-transfected and mock transfected ones. In addition, no difference was observed among the non-transfected cells, the mock-infected cells, and VEGF shRNA2, 3 and 4 transfected cells. * vs. control P<0.05; # vs. mock P<0.05.

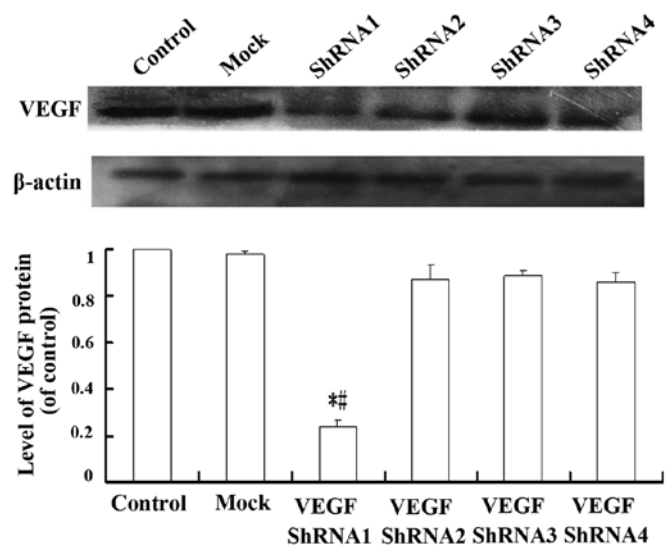


Figure 4. The level of VEGF protein was detected by western blot analysis 72 h after infection. The VEGF protein expression demonstrated a significant reduction in lentiviral vector-VEGF shRNA1 transfected C6GSCs, as compared with non-transfected cells and mock transfected cells. * vs. control P<0.05; # vs. mock P<0.05.

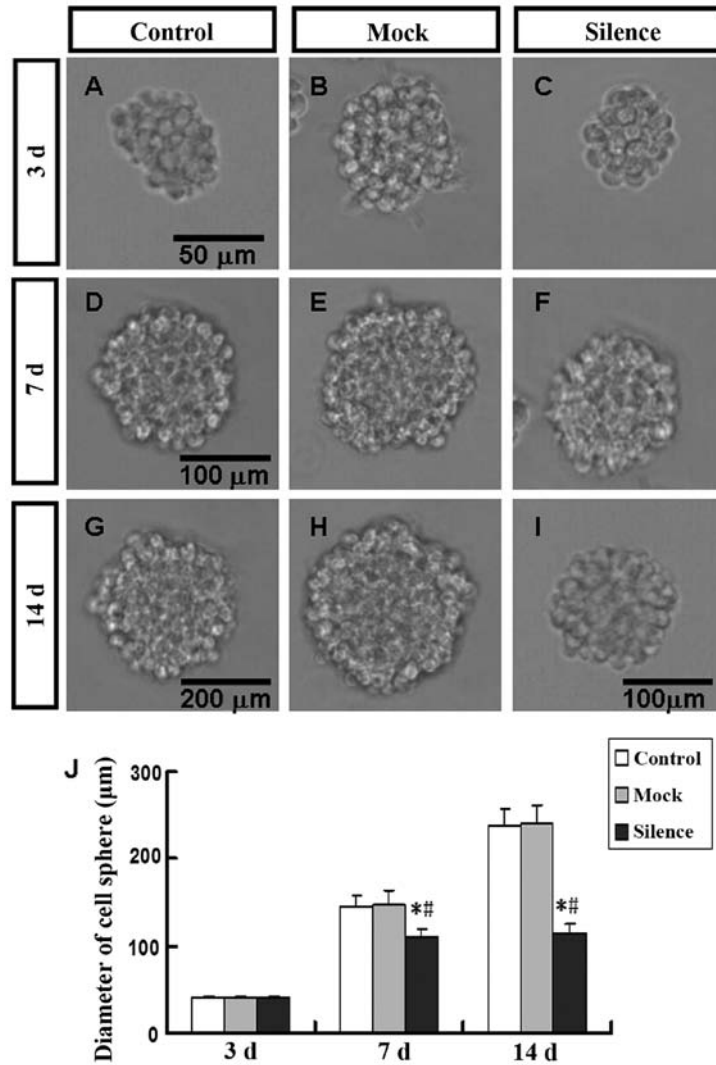


Figure 5. C6GSC sphere in the in serum-free NSC medium. Many C6 cells formed floating primary tumor spheres in serum-free NSC medium. (A-C) The sphere appearance of 3 groups is similar at 3 DIV, showing a small and uniform cell sphere. (D-J) In the following days in culture, the C6GSC spheres of control and mock group grew significantly faster and reached a larger size than that of the silence group. At 7 DIV, the proliferation of C6GSCs of the silence group reached the peak. On the contrary, C6GSCs of the other two groups proliferated continually and the diameter of a cell sphere was up to ~236.6820.43 and 240.8520.52 μm. * vs. control P<0.05; # vs. mock P<0.05.

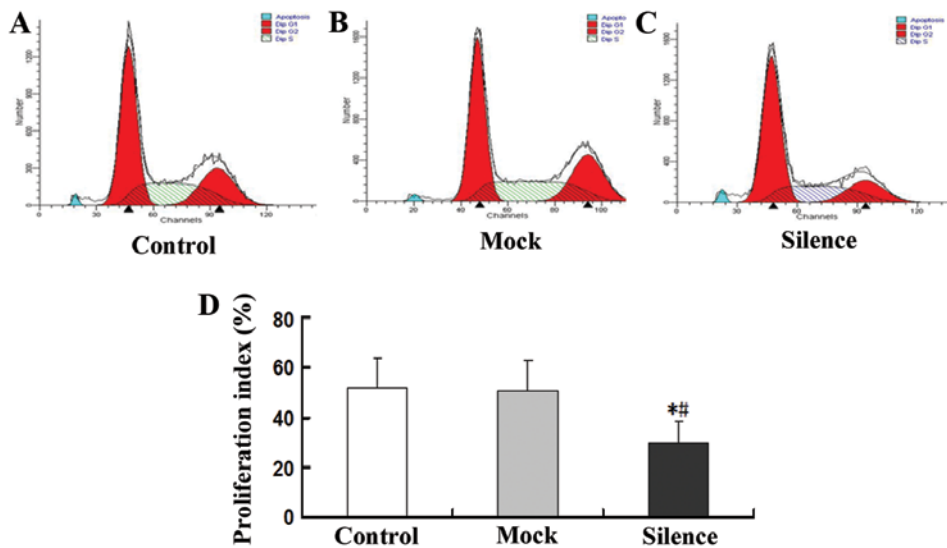


Figure 6. Proliferation of C6GSCs was evaluated by flow cytometry. The proliferation index of C6GSCs in the silence group was lower than that of the other two groups. # vs. mock P<0.05.

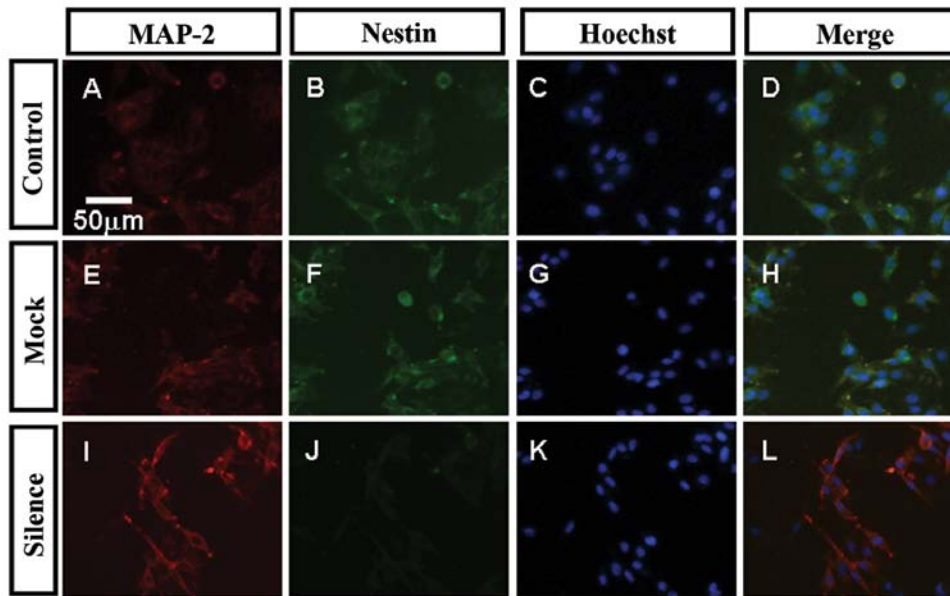


Figure 7. The differentiated neurons were detected by immunofluorescence after a 7-day differentiation culture. MAP-2 (red)-positive neurons in the silence group were nestin (green)-negative, cell morphology was good, showing extensive processes and rounded bodies. MAP-2-positive neurons in the other two groups were nestin-positive, cells morphology was less distinct.

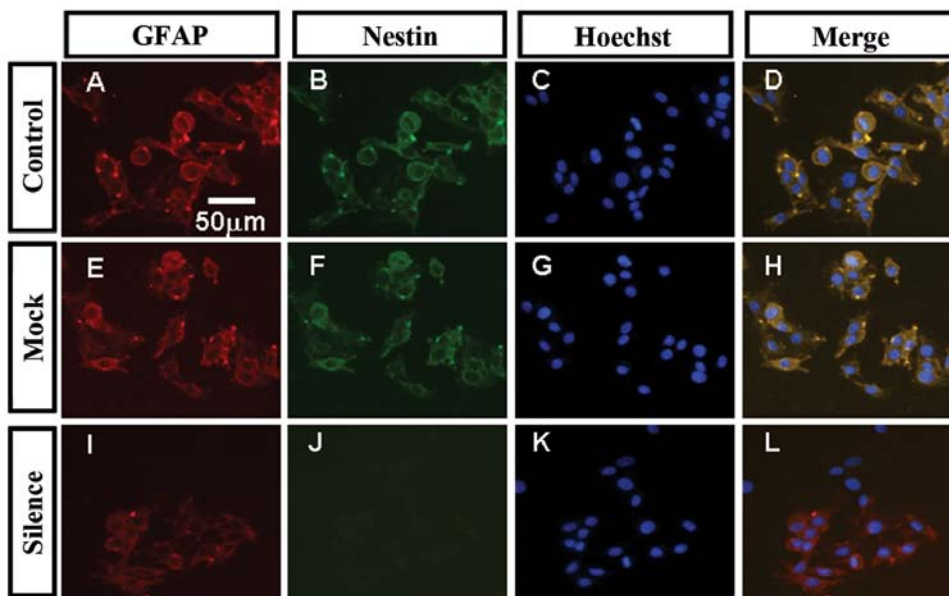


Figure 8. The differentiated astrocytes were detected by immunofluorescence after a 7-day differentiation culture. GFAP (red)-positive astrocytes in the silence group were nestin (green)-negative. GFAP-positive astrocytes in the other two groups were nestin-positive.

the contrary, the other two groups proliferated continually and the diameter of a cell sphere was up to $\sim 236.6820.43$ and $240.8520.52 \mu\text{m}$ (Fig. 5J). Flow cytometry also indicated that proliferation index of lentiviral vector-VEGF shRNA1 transfected C6GSCs were lower than that of the other two groups (Fig. 6).

Differentiation of C6GSCs. Differentiation culture of three kinds of stem cells was performed in the conditions outlined in Materials and methods. After 7 DIV, three kinds of

stem cells exhibited multi-directional differentiation, all of them differentiated into MAP-2-positive neurons and GFAP-positive astrocytes. MAP-2-positive neurons and GFAP-positive astrocytes derived from lentiviral vector-VEGF shRNA1 transfected C6GSCs were nestin-negative, cell morphology was good, showing extensive processes and rounded bodies. MAP-2-positive neurons and GFAP-positive astrocytes derived from the other two groups were nestin-positive, cell morphology was less distinct, the differentiated cells were poorly differentiated (Figs. 7 and 8).

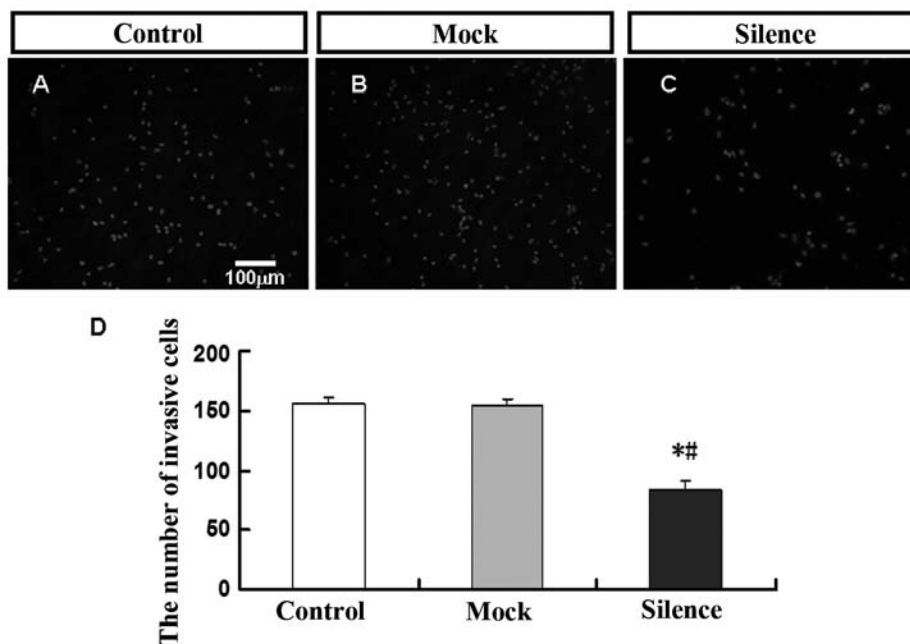


Figure 9. The invasion activity of C6GSCs was determined by Transwell chamber assay. After 12 h, the cells under the chamber were stained with Hoechst 33342. The invasive cells in the silence group were obviously decreased compared with the other two groups. However, there were no significant differences between the other two groups. * vs. control $P < 0.05$; # vs. mock $P < 0.05$.

Invasion of C6GSCs. Cell invasion is a characteristic feature of carcinoma cells. To investigate the role of VEGF in tumor cell invasion, we measured the ability of C6GSCs to invade through Matrigel-coated filters in a Transwell chamber assay. After transfected with VEGF shRNA1, the invasive cells were obviously decreased compared with the other two groups. However, there were no significant differences between the other two groups (Fig. 9).

Discussion

Gliomas are characterized by high morphological, genetic, and phenotypic heterogeneity. However, studies performed simply on bulk glioma cells yield limited information on its origin and the mechanisms which mediate its growth and progression. Encouragingly, by applying the methods used to study normal NSCs to brain tumor cells, many researcher have reported there were BTSCs in brain gliomas of different grades from both children and adults (26-31). BTSCs possess the ability to self-renew and to give rise to a variety of proliferating and differentiated cells that make up the brain tumor mass. BTSCs play an important role in resistance to radiotherapy and chemotherapy (32,33), angiogenesis (34) and metastasis (35). However, their source and molecular signal pathways are still not fully understood.

There have been only a few successful isolations of BTSCs from established cell lines such as the human U373, A172 and U87 glioma cell lines (36-38). Although the rat glioma cell line C6 is widely used in the study of gliomas, there is still controversy over the culture methods for BTSCs. The pioneering studies suggested cell surface markers such as CD133 (a cell surface marker for normal NSCs) and nestin (a cytoskeleton protein associated with NSCs and progenitor cells in central nervous system development) are recommended for the specific

identification of BTSCs (28,30,39,40). In this study, the C6 cell line was cultured in a simplified serum-free NSC medium, in which a fraction of C6 cells could form stem cell spheres. The C6GSC spheres were CD133 and nestin double-positive.

Direct evidence shows that gliomas and BTSCs express high levels of VEGF (8-11). In this study, RT-PCR and western blot analysis showed that also the C6GSCs could express VEGF. Traditionally, it is thought VEGF secreted by tumor cells interacts with VEGFRs expressed on the surface of tumor endothelial cells, but not on tumor cells (18-20) and promote the migration, growth and survival of endothelial cells (12-14). Recent studies suggest that tumor cells or BTSCs could express VEGFRs themselves (21-24). However, the direct effect of VEGF on biological behavior of BTSCs has not been completely elucidated.

We suggest that VEGF may be a key factor influencing the characteristics of C6GSCs. RNAi is highly specific and efficient in inhibiting target genes and is the focus of recent studies to make it a new tool for curing tumor, infectious and hereditary diseases (41). In this study, lentiviral vector-VEGF shRNA was constructed to target the VEGF genes in the C6GSCs. After 72-h transfection, the VEGF mRNA expression in lentiviral vector-VEGF shRNA1 transfected C6GSCs was reduced by ~75%. Compared to control and mock groups, the ability of cell proliferation of lentiviral vector-VEGF shRNA1 transfected C6GSCs was decreased significantly and GFAP, MAP-2-positive cells were nestin-negative, which indicated that the ability of differentiation was enhanced. After transfected with VEGF shRNA1, the invasive cells were obviously decreased compared with the other two groups through Matrigel-coated filters in a Transwell chamber assay. All the data demonstrate that downregulation of VEGF expression attenuates malignant biological behavior of C6GSCs. RNAi of VEGF expression implies an effective anti-glioma strategy.

References

1. Louis DN: Molecular pathology of malignant gliomas. *Annu Rev Pathol* 1: 97-117, 2006.
2. Rasper M, Schafer A, Piontek G, *et al*: Aldehyde dehydrogenase 1 positive glioblastoma cells show brain tumor stem cell capacity. *Neuro Oncol* 12: 1024-1033, 2010.
3. Folkman J: Role of angiogenesis in tumor growth and metastasis. *Semin Oncol* 29: 15-18, 2002.
4. Verhoeff JJ, van Tellingen O, Claes A, *et al*: Concerns about anti-angiogenic treatment in patients with glioblastoma multiforme. *BMC Cancer* 9: 444, 2009.
5. Keck PJ, Hauser SD, Krivi G, *et al*: Vascular permeability factor, an endothelial cell mitogen related to PDGF. *Science* 246: 1309-1312, 1989.
6. Leung DW, Cachianes G, Kuang WJ, Goeddel DV and Ferrara N: Vascular endothelial growth factor is a secreted angiogenic mitogen. *Science* 246: 1306-1309, 1989.
7. Takano S, Yoshii Y, Kondo S, *et al*: Concentration of vascular endothelial growth factor in the serum and tumor tissue of brain tumor patients. *Cancer Res* 56: 2185-2190, 1996.
8. Nishikawa R, Cheng SY, Nagashima R, Huang HJ, Cavenee WK and Matsutani M: Expression of vascular endothelial growth factor in human brain tumors. *Acta Neuropathol* 96: 453-462, 1998.
9. Berkman RA, Merrill MJ, Reinhold WC, *et al*: Expression of the vascular permeability factor/vascular endothelial growth factor gene in central nervous system neoplasms. *J Clin Invest* 91: 153-159, 1993.
10. Hamerlik P, Lathia JD, Rasmussen R, *et al*: Autocrine VEGF-VEGFR2-Neuropilin-1 signaling promotes glioma stem-like cell viability and tumor growth. *J Exp Med* 209: 507-520, 2012.
11. He H, Niu CS and Li MW: Correlation between glioblastoma stem-like cells and tumor vascularization. *Oncol Rep* 27: 45-50, 2012.
12. Gu Q, Wang D, Wang X, *et al*: Basic fibroblast growth factor inhibits radiation-induced apoptosis of HUVECs. I. The PI3K/AKT pathway and induction of phosphorylation of BAD. *Radiat Res* 161: 692-702, 2004.
13. Gingis-Velitski S, Zetser A, Flugelman MY, Vlodayvsky I and Ilan N: Heparanase induces endothelial cell migration via protein kinase B/Akt activation. *J Biol Chem* 279: 23536-23541, 2004.
14. Gerber HP, McMurtrey A, Kowalski J, *et al*: Vascular endothelial growth factor regulates endothelial cell survival through the phosphatidylinositol 3'-kinase/Akt signal transduction pathway. Requirement for Flk-1/KDR activation. *J Biol Chem* 273: 30336-30343, 1998.
15. de Vries C, Escobedo JA, Ueno H, Houck K, Ferrara N and Williams LT: The fms-like tyrosine kinase, a receptor for vascular endothelial growth factor. *Science* 255: 989-991, 1992.
16. Millauer B, Wizigmann-Voos S, Schnurch H, *et al*: High affinity VEGF binding and developmental expression suggest Flk-1 as a major regulator of vasculogenesis and angiogenesis. *Cell* 72: 835-846, 1993.
17. Terman BI, Dougher-Vermazen M, Carrion ME, *et al*: Identification of the KDR tyrosine kinase as a receptor for vascular endothelial cell growth factor. *Biochem Biophys Res Commun* 187: 1579-1586, 1992.
18. Plate KH, Breier G, Weich HA, Mennel HD and Risau W: Vascular endothelial growth factor and glioma angiogenesis: coordinate induction of VEGF receptors, distribution of VEGF protein and possible in vivo regulatory mechanisms. *Int J Cancer* 59: 520-529, 1994.
19. Norden AD, Drappatz J and Wen PY: Antiangiogenic therapies for high-grade glioma. *Nat Rev Neurol* 5: 610-620, 2009.
20. Iwamoto FM and Fine HA: Bevacizumab for malignant gliomas. *Arch Neurol* 67: 285-288, 2010.
21. Gorski DH, Beckett MA, Jaskowiak NT, *et al*: Blockage of the vascular endothelial growth factor stress response increases the antitumor effects of ionizing radiation. *Cancer Res* 59: 3374-3378, 1999.
22. Graeven U, Fiedler W, Karpinski S, *et al*: Melanoma-associated expression of vascular endothelial growth factor and its receptors FLT-1 and KDR. *J Cancer Res Clin Oncol* 125: 621-629, 1999.
23. Knizetova P, Ehrmann J, Hlobilkova A, *et al*: Autocrine regulation of glioblastoma cell cycle progression, viability and radioresistance through the VEGF-VEGFR2 (KDR) interplay. *Cell Cycle* 7: 2553-2561, 2008.
24. Hlobilkova A, Ehrmann J, Knizetova P, Krejci V, Kalita O and Kolar Z: Analysis of VEGF, Flt-1, Flk-1, nestin and MMP-9 in relation to astrocytoma pathogenesis and progression. *Neoplasma* 56: 284-290, 2009.
25. Kabos P, Ehtesham M, Kabosova A, Black KL and Yu JS: Generation of neural progenitor cells from whole adult bone marrow. *Exp Neurol* 178: 288-293, 2002.
26. Ignatova TN, Kukekov VG, Laywell ED, Suslov ON, Vrionis FD and Steindler DA: Human cortical glial tumors contain neural stem-like cells expressing astroglial and neuronal markers in vitro. *Glia* 39: 193-206, 2002.
27. Hemmati HD, Nakano I, Lazareff JA, *et al*: Cancerous stem cells can arise from pediatric brain tumors. *Proc Natl Acad Sci USA* 100: 15178-15183, 2003.
28. Singh SK, Clarke ID, Terasaki M, *et al*: Identification of a cancer stem cell in human brain tumors. *Cancer Res* 63: 5821-5828, 2003.
29. Galli R, Binda E, Orfanelli U, *et al*: Isolation and characterization of tumorigenic, stem-like neural precursors from human glioblastoma. *Cancer Res* 64: 7011-7021, 2004.
30. Singh SK, Hawkins C, Clarke ID, *et al*: Identification of human brain tumour initiating cells. *Nature* 432: 396-401, 2004.
31. Yuan X, Curtin J, Xiong Y, *et al*: Isolation of cancer stem cells from adult glioblastoma multiforme. *Oncogene* 23: 9392-9400, 2004.
32. Beier D, Hau P, Proescholdt M, *et al*: CD133(+) and CD133(-) glioblastoma-derived cancer stem cells show differential growth characteristics and molecular profiles. *Cancer Res* 67: 4010-4015, 2007.
33. Bao S, Wu Q, McLendon RE, *et al*: Glioma stem cells promote radioresistance by preferential activation of the DNA damage response. *Nature* 444: 756-760, 2006.
34. Dean M, Fojo T and Bates S: Tumour stem cells and drug resistance. *Nat Rev Cancer* 5: 275-284, 2005.
35. Bao S, Wu Q, Sathornsumetee S, *et al*: Stem cell-like glioma cells promote tumor angiogenesis through vascular endothelial growth factor. *Cancer Res* 66: 7843-7848, 2006.
36. Kang SK, Park JB and Cha SH: Multipotent, dedifferentiated cancer stem-like cells from brain gliomas. *Stem Cells Dev* 15: 423-435, 2006.
37. Patrawala L, Calhoun T, Schneider-Broussard R, Zhou J, Claypool K and Tang DG: Side population is enriched in tumorigenic, stem-like cancer cells, whereas ABCG2+ and ABCG2- cancer cells are similarly tumorigenic. *Cancer Res* 65: 6207-6219, 2005.
38. Yu SC, Ping YF, Yi L, *et al*: Isolation and characterization of cancer stem cells from a human glioblastoma cell line U87. *Cancer Lett* 265: 124-134, 2008.
39. Shen G, Shen F, Shi Z, *et al*: Identification of cancer stem-like cells in the C6 glioma cell line and the limitation of current identification methods. *In Vitro Cell Dev Biol Anim* 44: 280-289, 2008.
40. Zhou XD, Wang XY, Qu FJ, *et al*: Detection of cancer stem cells from the C6 glioma cell line. *J Int Med Res* 37: 503-510, 2009.
41. Jain RK: Normalizing tumor vasculature with anti-angiogenic therapy: a new paradigm for combination therapy. *Nat Med* 7: 987-989, 2001.